

# NJC

Accepted Manuscript



This article can be cited before page numbers have been issued, to do this please use: M. Fang, L. Shao, T. Shi, Y. Chen, H. Yu, P. Li, W. Wang and B. Zhao, *New J. Chem.*, 2018, DOI: 10.1039/C8NJ02161A.



This is an Accepted Manuscript, which has been through the Royal Society of Chemistry peer review process and has been accepted for publication.

Accepted Manuscripts are published online shortly after acceptance, before technical editing, formatting and proof reading. Using this free service, authors can make their results available to the community, in citable form, before we publish the edited article. We will replace this Accepted Manuscript with the edited and formatted Advance Article as soon as it is available.

You can find more information about Accepted Manuscripts in the [author guidelines](#).

Please note that technical editing may introduce minor changes to the text and/or graphics, which may alter content. The journal's standard [Terms & Conditions](#) and the ethical guidelines, outlined in our [author and reviewer resource centre](#), still apply. In no event shall the Royal Society of Chemistry be held responsible for any errors or omissions in this Accepted Manuscript or any consequences arising from the use of any information it contains.

# Four Tetra-nuclear Lanthanide Complexes based on 8-hydroxyquinolin derivatives: Magnetic refrigeration and Single-Molecule Magnet behaviour†

Ming Fang,<sup>a,\*</sup> Li-Jun Shao,<sup>a</sup> Tian-Xing Shi,<sup>a</sup> Ying-Ying Chen,<sup>a</sup> Hong Yu,<sup>a</sup> Peng-Fei Li,<sup>a</sup> Wen-Min Wang<sup>b,\*</sup> Bin Zhao<sup>c,\*</sup>

## Abstract:

Four tetra-nuclear lanthanide complexes:  $\{[\text{Ln}_4(\text{L})_6(\text{tmhd})_4(\mu_3\text{-OH})_2]\cdot\text{mH}_2\text{O}\}$  ( $\text{Ln} = \text{Gd}$  (**1**,  $m = 0$ ),  $\text{Tb}$  (**2**,  $m = 3$ ),  $\text{Dy}$  (**3**,  $m = 0$ ),  $\text{Ho}$  (**4**,  $m = 0$ );  $\text{L} = 5\text{-}((\text{pyridin-4-ylmethylene})\text{amino})\text{quinolin-8-ol}$ ,  $\text{tmhd} = 2,2,6,6\text{-tetramethylheptane-3,5-dione}$ ) were fabricated and structurally characterized. Compounds **1-4** are isostructural belonging to the monoclinic system with space group  $P2_1/n$ . The core of the complexes contain a tetranuclear arrangement of  $\text{Ln}^{\text{III}}$  ions which is bridged by two pyramidal  $\mu_3\text{-OH}^-$  ions, and the four  $\text{Ln}^{\text{III}}$  ions are precisely coplanar. Magnetic study reveals that **1** exhibits cryogenic magnetic refrigeration property ( $-\Delta S_m = 20.85 \text{ J K}^{-1} \text{ kg}^{-1}$ ), whereas compound **3** exhibits slow relaxation of the magnetization.

**Keyword:** Lanthanide, Tetra-nuclear compounds, Magnetocaloric effect, Single-molecule magnet behaviour, 8-hydroxyquinolin derivatives

## Introduction

There is no doubt that the investigation of lanthanide (III) complexes is a highly

*a* Department of Chemistry, Hebei Normal University of Science & Technology, Qinhuangdao 066004, Hebei province, P. R.China. E-mail:fangmingchem@163.com

*b* Department of Chemistry, Taiyuan Normal University, Jinzhong 030619, PR China. E-mail: wangwenmin0506@126.com

*c* Department of Chemistry, Key Laboratory of Advanced Energy Material Chemistry, MOE, and TKL of Metal and Molecule Based Material Chemistry, Nankai University, Tianjin 300071, China.. E-mail: zhaobin@nankai.edu.cn

† Electronic supplementary information (ESI) available: Selected bond lengths and angles. CCDC 1830533-1830536. For ESI and crystallographic data in CIF or other electronic format see DOI: 10.1039/c000000x/

active research topic due to their employment in luminescence,<sup>[1]</sup> magnetism,<sup>[2]</sup> gas adsorption and separation,<sup>[3]</sup> catalysis,<sup>[4]</sup> and so on. Among above potential applications, the study of single molecule magnets (SMMs) and molecular magnetic refrigeration attract innumerable attentions.<sup>[5,6]</sup> Since  $\text{Mn}_{12}\text{O}_{12}(\text{O}_2\text{CCH}_3)_{16}(\text{H}_2\text{O})_4$ <sup>[7]</sup> which behaves as a magnet at the molecular level, was reported, the study of bistable molecular magnetic materials is a highly active research topic in the chemistry and physics communities due to their potential applications in high density magnetic data storage and spintronic devices<sup>[8]</sup> and quantum computing.<sup>[9]</sup> Subsequently, numerous new Ln(III)-based molecules behaving as SMMs were discovered over the last decades, and display excellent and interesting magnetic behaviors. Lately, the record of effective energy barrier ( $U_{\text{eff}}$ ) has been broken continually, and not long ago a mononuclear Dy (III) compound with the  $U_{\text{eff}}$  as large as 1025 K was reported by Tong and co-worker;<sup>[10]</sup> shortly afterwards, the group of Zheng reports a nearly perfect pentagonal bipyramidal Dy compound with the largest effective energy barrier  $U_{\text{eff}} = 1815 \text{ K}$ ,<sup>[11a]</sup> recently, Layfield group reported a dysprosium metallocene with a largest energy barrier  $U_{\text{eff}} = 1837 \text{ K}$ , setting a new record in this field.<sup>[11b]</sup> These important reports attract more and more researcher to focus on the study of SMMs.

Molecular magnetic coolers, which are based on the magnetocaloric effect (MCE), are another research focus. Due to the environmental safety and energy efficiency, magnetocaloric materials have been proposed to replace the expensive and increasingly rare He-3 in ultralow temperature refrigeration.<sup>[12]</sup> In general, an outstanding molecular magnetic cooler should bear the features of a large spin ground state  $S$ , negligible magnetic anisotropy, dominant ferromagnetic interaction and high magnetic density.<sup>[13]</sup> Thus,  $\text{Gd}^{3+}$  is a common constituent element for molecular refrigerant materials, because it is favored by it having a  $^8\text{S}_{7/2}$  ground-state term ( $S=7/2$ ,  $L=0$ ), with high spin and zero orbital momentum, and therefore no spin-orbit coupling is possible. To date, a large number of impressive compounds associated with molecular magnetic cooling have been reported, and the largest record of  $-\Delta S_{\text{m}}$  has been broken frequently.<sup>[14]</sup>

Therefore, there is a continuing need to search for new molecular systems that

have improved magnetic properties for better understanding and practical applications. In this contribution, four tetranuclear lanthanide complexes with a general formula  $\{[Ln_4(L)_6(tmhd)_4(\mu_3-OH)_2] \cdot mH_2O\}$  ( $Ln = Gd$  (**1**,  $m = 0$ ),  $Tb$  (**2**,  $m = 3$ ),  $Dy$  (**3**,  $m = 0$ ),  $Ho$  (**4**,  $m = 0$ );  $L = 5-((pyridin-4-ylmethylene)amino)quinolin-8-ol$ ,  $tmhd = 2,2,6,6-tetramethylheptane-3,5-dione$ ) were fabricated and structurally characterized. Magnetic study reveals that **1** exhibits cryogenic magnetic refrigeration property, whereas compound **3** exhibits slow relaxation of the magnetization.

## Experimental section

### Materials and Physical Measurements.

All chemicals purchased were of reagent grade and used without further purification. Water used in the reactions is distilled water. Analyses for C, H and N were carried out on a Perkin-Elmer analyzer. Powder X-ray diffraction measurements were recorded on a Rigaku Ultima IV instrument using  $Cu K\alpha$  radiation ( $\lambda = 1.54056 \text{ \AA}$ ), with a scan speed of  $5^\circ \text{ min}^{-1}$  in the range of  $2\theta = 5-50^\circ$ . Magnetic susceptibilities were performed on a Quantum Design PPMS-9 ACMS magnetometer. Diamagnetic corrections were made with Pascal's constants for all the constituent atoms.

### Crystallographic studies.

Single-crystal X-ray diffraction measurements of **1 - 4** were carried out at room temperature on a Rigaku Saturn724 CCD X-ray diffractometer equipped with graphite monochromated  $MoK\alpha$  radiation ( $\lambda = 0.71073 \text{ \AA}$ ). Lorentz polarization and absorption corrections were applied. The structures were solved by direct methods and refined by full-matrix least-squares techniques using the SHELXS-97 and SHELXL-97 programs.<sup>[15]</sup> All the nonhydrogen atoms were refined with anisotropic parameters while H atoms were placed in calculated positions and refined using a riding model. Crystallographic data for **1 - 4** were summarized in Table 1. Selected bond lengths and angles were summarized in Table S1-S4.

### Synthesis of 5-aminoquinolin-8-ol.

A mixture of 5-nitroquinolin-8-ol (50 mmol) and 5 % Pd/C (0.75 g), which was used as catalyst, in a 1.3 % ratio in absolute isopropanol was heated to  $65^\circ C$ , and

then 12 mL of 85 % hydrazine hydrate was dropped into the mixture over 1 h. It was heated to 90 °C and refluxed for 6 h. Finally, the solvent was removed, and dichloromethane was used to wash the grass green solid product (yield: 50.8%). Elemental analysis (%): Calcd for C<sub>9</sub>H<sub>8</sub>ON<sub>2</sub> (F<sub>w</sub> = 160.42): C 67.32, H 5.00, N 17.50. Found: C 67.28, H 4.97, N 17.82.

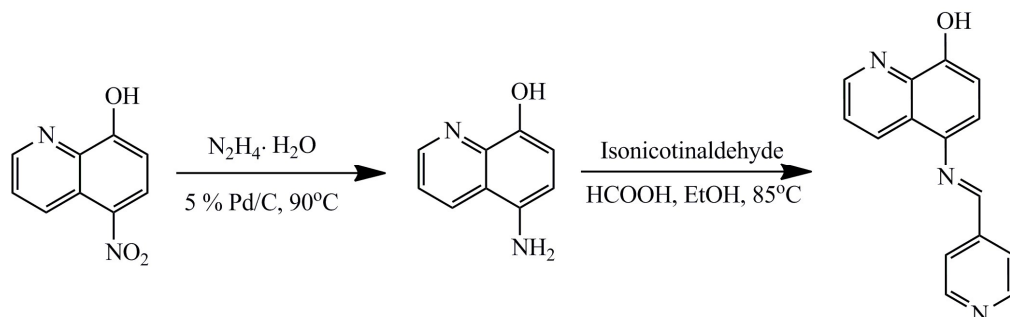
**Table 1.** Crystallographic Data and Structure Refinements for **1-4**

	<b>1</b>	<b>2</b>	<b>3</b>	<b>4</b>
formula	C <sub>134</sub> H <sub>138</sub> N <sub>18</sub> O <sub>16</sub> Gd <sub>4</sub>	C <sub>134</sub> H <sub>144</sub> N <sub>18</sub> O <sub>19</sub> Tb <sub>4</sub>	C <sub>134</sub> H <sub>138</sub> N <sub>18</sub> O <sub>16</sub> Dy <sub>4</sub>	C <sub>134</sub> H <sub>138</sub> N <sub>18</sub> O <sub>16</sub> Ho <sub>4</sub>
<i>Mr</i> (g mol <sup>-1</sup> )	2885.62	2946.35	2906.62	2916.34
<i>T</i> (K)	293(2)	133(2)	293(2)	149.99
cryst syst	monoclinic	monoclinic	monoclinic	monoclinic
Space group	<i>P</i> 21/ <i>n</i>	<i>P</i> 21( <i>1</i> )/ <i>n</i>	<i>P</i> 21/ <i>n</i>	<i>P</i> 21/ <i>n</i>
<i>a</i> (Å)	19.1634(7)	18.975(3)	18.9972(7)	19.1765(13)
<i>b</i> (Å)	17.2152(6)	17.373(2)	17.3458(6)	17.1770(11)
<i>c</i> (Å)	22.4329(8)	22.320(3)	22.3245(8)	22.4477(14)
$\alpha$ (°)	90	90	90	90
$\beta$ (°)	114.6210(10)	114.548(4)	114.8280(10)	114.520(2)
$\gamma$ (°)	90	90	90	90
<i>V</i> (Å <sup>3</sup> )	6727.8(4)	6692.8(17)	6676.5(4)	6727.3(8)
<i>Z</i>	2	2	2	2
cryst size (mm <sup>3</sup> )	0.35 x 0.24 x 0.11	0.20×0.18×0.14	0.25 x 0.14 x 0.11	0.32 x 0.23 x 0.13
<i>D<sub>c</sub></i> (g cm <sup>-3</sup> )	1.424	1.462	1.446	1.440
$\mu$ (mm <sup>-1</sup> )	2.013	2.158	2.280	2.393
<i>R<sub>int</sub></i>	0.0540	0.0466	0.0426	0.0742
limiting indices	-22≤ <i>h</i> ≤22, -20≤ <i>k</i> ≤20, -26≤ <i>l</i> ≤26	-22≤ <i>h</i> ≤22, -17≤ <i>k</i> ≤20, -26≤ <i>l</i> ≤26	-22≤ <i>h</i> ≤22, -20≤ <i>k</i> ≤20, -26≤ <i>l</i> ≤26	-22≤ <i>h</i> ≤22, -20≤ <i>k</i> ≤20, -26≤ <i>l</i> ≤26
reflns collected	76780	57351	125364	82176
params	828	946	813	768
GOF on <i>F</i> <sup>2</sup>	1.079	1.051	1.062	1.083
<i>R<sub>I</sub></i> , <i>wR</i> <sub>2</sub> [ <i>I</i> > 2σ( <i>I</i> )]	0.0310, 0.0693	0.0324, 0.0981	0.0311, 0.0721	0.0543, 0.1188
<i>R<sub>I</sub></i> , <i>wR</i> <sub>2</sub> (all data)	0.0483, 0.0789	0.0362, 0.1003	0.0417, 0.0788	0.0738, 0.1310

### Synthesis of 5-((pyridin-4-ylmethylene)amino)quinolin-8-ol (HL)

The Schiff base ligand 5-((pyridin-4-ylmethylene)amino)quinolin-8-ol (HL) was synthesized in a simple aldimine condensation reaction of 5-aminoquinolin-8-ol (10 mmol) with isonicotinaldehyde (10 mmol) in 50 mL ethanol with the catalyze of 5 drops formic acid (Scheme 1). The reaction mixture was stirred for 5 h at 85 °C. The

product was isolated from the mixture and it was purified by recrystallization from a mixed solvent of ethanol and acetone (3/1, v/v). The purified product was obtained as a green solid (yield 2.1 g, 80.2%).



Scheme 1. The synthesis of HL.

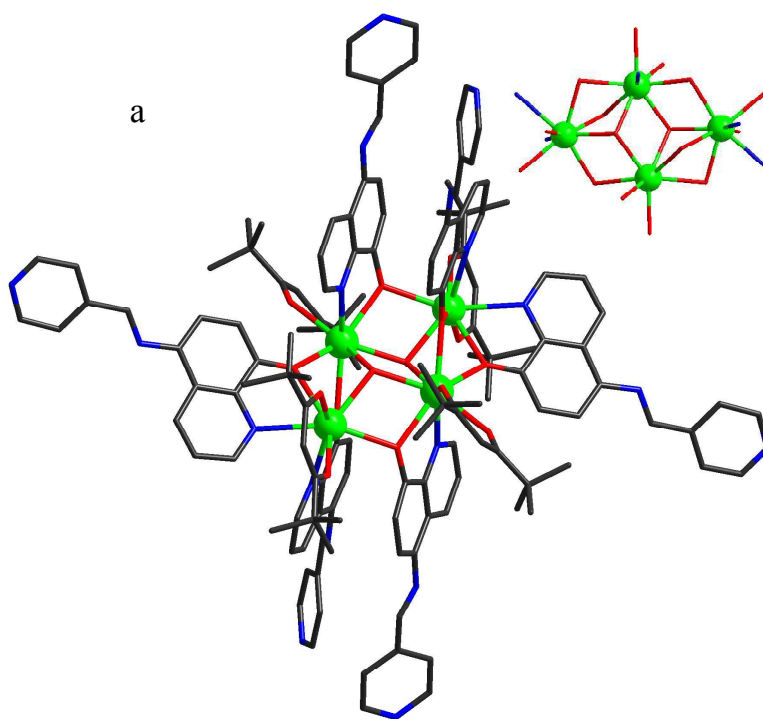
### Synthesis of Complexes 1–5

The compounds **1–4** were obtained by the reaction of  $\text{Ln}(\text{tmhd})_3 \cdot 2\text{H}_2\text{O}$  (0.025 mmol;  $\text{Ln}(\text{III}) = \text{Gd}$  (**1**),  $\text{Tb}$  (**2**),  $\text{Dy}$  (**3**),  $\text{Ho}$  (**4**)) and HL (0.025 mmol) in mixture solution containing 20 mL acetonitrile and 3 mL  $\text{CH}_2\text{Cl}_2$ . The ensuing yellow solution was stirred at room temperature for about 4 h. After filtration, the resultant solution was left unperturbed to evaporate slowly. Yellow block shaped crystals suitable for single-crystal X-ray data collection was isolated after about 5 days. Yield: 52%, 45%, 56% and 48% based on HL for **1–4**, respectively. Elemental analysis calcd (%) for  $\text{C}_{134}\text{H}_{138}\text{N}_{18}\text{O}_{16}\text{Gd}_4$  (**1**): C 55.77, H 4.82, N 8.74; found: C 55.62, H 4.87, N 8.68; for  $\text{C}_{134}\text{H}_{144}\text{N}_{18}\text{O}_{19}\text{Tb}_4$  (**2**): C 54.62, H 4.93, N 8.56; found: C 54.74, H 4.89, N 8.62; for  $\text{C}_{134}\text{H}_{138}\text{N}_{18}\text{O}_{16}\text{Dy}_4$  (**3**): C 55.37, H 4.79, N 8.67; found: C 55.35, H 4.64, N 8.71; for  $\text{C}_{134}\text{H}_{138}\text{N}_{18}\text{O}_{16}\text{Ho}_4$  (**4**): C 55.19, H 4.77, N 8.65; found: C 55.27, H 4.89, N 8.57. The IR spectra of **1–4** are given in electronic supplementary information (Figure S1–S4).

### Results and Discussion

Single crystal X-ray diffraction reveals that the four compounds are isostructural, crystallizing in the monoclinic space group  $P2_1/n$  (Table 1), with  $Z = 2$ . The structure of **3** ( $\text{Ln} = \text{Dy}$ ) will be described here as a representative example of the series. The core of the complex (Figure 1a) contains a tetranuclear arrangement of  $\text{Dy}^{\text{III}}$  ions with crystallographic inversion symmetry. The four  $\text{Dy}^{\text{III}}$  ions are precisely coplanar

(Figure 1b), bridged by the two O-atoms derived from pyramidal  $\mu_3$ -OH<sup>-</sup> ions (O2), with the Dy-O2 distances 2.338(3), 2.408(3) and 2.328(3) Å, and the Dy-O2-Dy angles 112.35(12), 99.05(11) and 107.54(11)°, and a Dy—Dy distance of 3.6033(3), 3.8764(3) and 3.8285(4) Å. The two oxygen atoms (O2) of the  $\mu_3$ -OH<sup>-</sup> ligands are located on opposite sides of the Dy<sub>4</sub> plane and are displaced out of that plane by 0.904 Å. Dy1 is chelated by two oxygen atoms of tmhd<sup>-</sup> ligand and two independent L<sup>-</sup> ligands *via* the pyridyl nitrogen and the phenoxy oxygen atoms, which connect to Dy2. Dy1 also coordinate with another phenoxy oxygen atoms which bridge with Dy2, and one  $\mu_3$  oxygen atoms. Dy2 is coordinated with two bridging phenoxy oxygen atoms, two  $\mu_3$  oxygen atoms, and chelated by one tmhd<sup>-</sup> and one independent L<sup>-</sup> ligand. Both Dy1 and Dy2 are eight-coordinated, and the coordination geometry for the eight-coordinated Dy1 and Dy2 can be described as a distorted bicapped trigonal prism (Figure S5). The coordination and bridging modes of the ligands are shown in Scheme 2. The Dy-O bond lengths are in the range of 2.285(3)- 2.408(3) Å. The Dy-N bond lengths are 2.533(3), 2.587(4) and 2.536(4) Å.



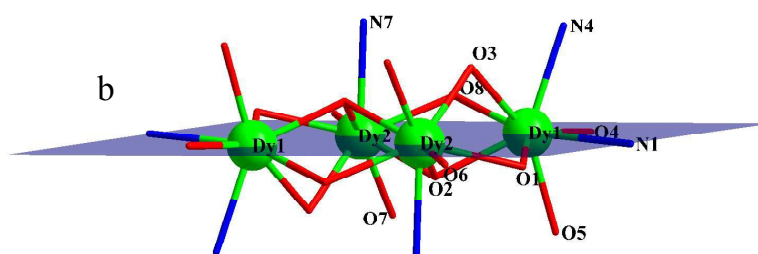
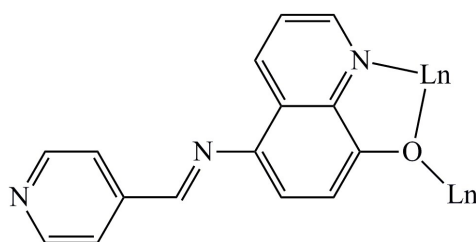


Figure 1. Perspective view (a) and side view (core only) (b) of **3** (all hydrogen atoms are omitted for clarity).



Scheme 2. Coordination Modes of  $L^-$  ligand.

The average Ln-O bond lengths (Å) for **1–4** were listed in Table 2. These values are comparable to those of the already reported lanthanide complexes.<sup>[16]</sup> The average Ln-O distances display a decrease trend with the increase of atomic number from Gd to Ho, demonstrating the existence of lanthanide contraction effect.<sup>[17]</sup>

Table 2. The statistical data of bond lengths (Å) and angles (°) for **1–4**.

Complexes	The range of Ln–O bond lengths / Å	Average Ln–O bond lengths / Å
<b>1Gd</b>	2.317(3)–2.451(3)	2.387(3)
<b>2Tb</b>	2.300(2)–2.427(2)	2.371(5)
<b>3Dy</b>	2.284(3)–2.411(3)	2.361(3)
<b>4Ho</b>	2.315(5)–2.444(4)	2.385(4)

### Powder X-ray diffraction (PXRD)

The purity of crystalline powders of **1–4** were confirmed by powder X-ray diffraction (PXRD) (Figure S6), the experimental PXRD patterns are consistent with the corresponding simulated from the single crystal data, suggesting the phase purity of the samples.



## Luminescence properties of **2**

The solid-state luminescence property of **2** was investigated at the exciting wavelength of 305 nm at room temperature. As shown in Figure S7, the emission spectrum of **2** exhibits the characteristic emissions of Tb<sup>III</sup> ion. The emission spectrum presents four peaks at 491, 546, 587 and 621 nm which are assigned to the transition of <sup>5</sup>D<sub>4</sub> to <sup>7</sup>F<sub>J</sub> (*J* = 6, 5, 4, 3). Among them, the emission peak at 546 nm (<sup>5</sup>D<sub>4</sub>→<sup>7</sup>F<sub>5</sub>) is clearly stronger than the other three ones.

## Magnetic Properties of **1-4**

The magnetic susceptibilities of **1-4** were measured on the microcrystalline samples in the temperature range from 2 to 300 K and under 1000 Oe field, as shown in Figure 2. At room temperature, the  $\chi_M T$  value for **1-4** is 31.73, 47.46, 56.52 and 56.27 cm<sup>3</sup> K mol<sup>-1</sup>, respectively, which is close to the corresponding theoretical value of 31.52, 47.28, 56.68 and 56.28 cm<sup>3</sup> K mol<sup>-1</sup> expected for four magnetically Ln<sup>3+</sup> ions: Gd<sup>3+</sup> in the <sup>8</sup>S<sub>7/2</sub> ground state (*g* = 2) for **1**, Tb<sup>3+</sup> in the <sup>7</sup>F<sub>6</sub> ground state (*g* = 3/2) for **2**, Dy<sup>3+</sup> in the <sup>6</sup>H<sub>15/2</sub> ground state (*g* = 4/3) for **3** and Ho<sup>3+</sup> in the <sup>5</sup>I<sub>8</sub> ground state (*g* = 5/4) for **4**. For **1**, the  $\chi_M T$  value stays almost constant in the temperature range 300–25 K and then decreases rapidly to a minimum value of 18.98 cm<sup>3</sup> K mol<sup>-1</sup> at 2 K, which indicates the presence of a weak antiferromagnetic interaction between the adjacent Gd<sup>3+</sup> ions. Based on the Hamiltonian  $\hat{H} = -J\hat{S}_A\hat{S}_B$  with  $\hat{S}_A = \hat{S}_B = 7/2$ , a corresponding equation as following was deduced, and the magnetic properties of **1** can be appropriately described by it.<sup>[18]</sup>

$$\chi_M = 2 * \frac{2Ng^2\beta^2}{kT} \times \frac{e^{J/kT} + 5e^{3J/kT} + 14e^{6J/kT} + 30e^{10J/kT} + 55e^{15J/kT} + 91e^{21J/kT} + 140e^{28J/kT}}{1 + 3e^{J/kT} + 5e^{3J/kT} + 7e^{6J/kT} + 9e^{10J/kT} + 11e^{15J/kT} + 13e^{21J/kT} + 15e^{28J/kT}}$$

Least-squares fitting of the experimental data leads to *J* = -0.14 cm<sup>-1</sup>, *g* = 1.98, and the agreement factor *R*, defined as  $R = \sum(\chi_{\text{obsd}} - \chi_{\text{calcd}})^2 / \sum(\chi_{\text{obsd}})^2$ , is 4.8×10<sup>-1</sup>. The negative and small *J* value indicates very weak antiferromagnetic coupling interaction between adjacent Gd<sup>3+</sup>. For lanthanide ions, the 4f electrons are well shielded by outer-shell electrons, compared with 3d electrons, the interaction of 4f electrons from adjacent lanthanide ions is rather weak.

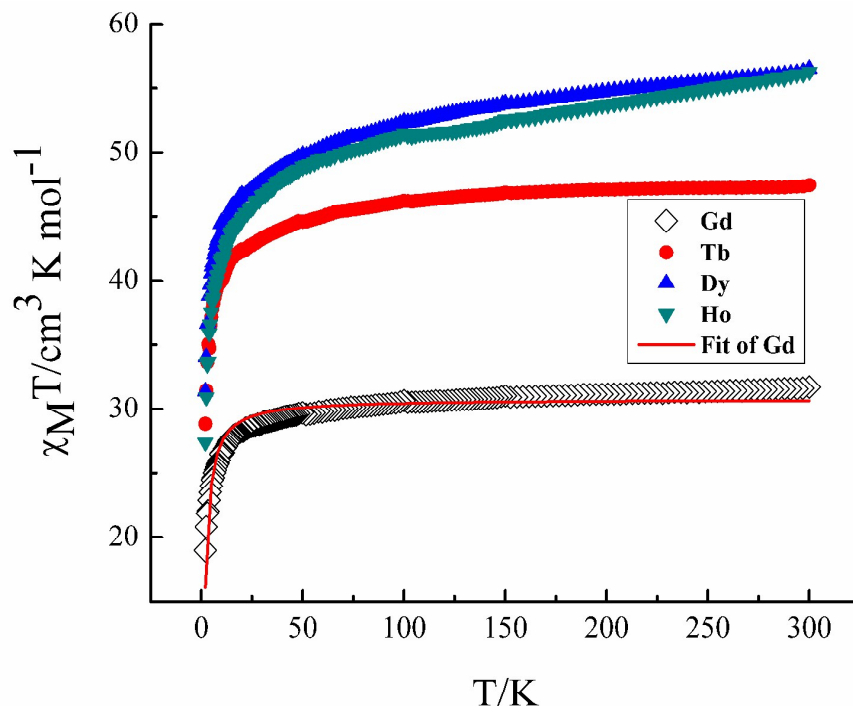


Figure 2 The plots of  $\chi_M T$  versus  $T$  for **1**( $\diamond$ ), **2**( $\bullet$ ), **3**( $\blacktriangle$ ) and **4**( $\blacktriangledown$ ) under 1000 Oe field.

For **2-4**, as the temperature is lowered,  $\chi_M T$  values decrease slightly to 25 K, then decrease quickly to 28.84, 31.40 and 27.39  $\text{cm}^3 \text{K mol}^{-1}$ , respectively. The decrease observed in the  $\chi_M T$  values is most likely due to a combination of some very weak antiferromagnetic interactions between adjacent lanthanide ions and/or the thermal depopulation of Stark sublevels.<sup>[19]</sup>

The magnetization data of **1** is performed at a field of 0–8 T between 2 and 10 K. As shown in Figure 4, the  $M$  versus  $H$  curves display a gradual increase with the increasing field and saturation values of  $28.19 N\beta$  for **1** at 80 kOe and 2 K, which is extremely close to the theoretical value of  $28 N\beta$  for four individual Gd(III) ( $S = 7/2$ ,  $g = 2$ ) ions. Magnetic entropy changes  $\Delta S_m$  of **1** can be calculated from the  $M$  versus  $H$  data to evaluate the MCE.  $\Delta S_m$  are calculated by using the Maxwell equation:

$$\Delta S_m(T) = \int [\partial M(T, H)/\partial T] H dH \quad (1)$$

According to eq 1,<sup>[20]</sup> the  $-\Delta S_m$  values of **1** can be obtained; the plots of  $-\Delta S_m$  versus  $T$  are shown in Figure 3 (Right). For **1**, the maximum value of  $-\Delta S_m$  is  $20.85 \text{ J K}^{-1} \text{ kg}^{-1}$  (calculated as  $4R\ln(2S+1)$ ), expected maximum  $-\Delta S_m$  is  $23.97 \text{ J K}^{-1} \text{ kg}^{-1}$  for a

field change  $\Delta H = 7$  T at 2.0 K. The difference of  $-\Delta S_m$  between the experimental and theoretical values for **1** might be due to the antiferromagnetic interaction in **1**.<sup>[21]</sup> The maximum  $-\Delta S_m$  of **1** is smaller than the antiferromagnetic  $\{Gd_4\}$  complexes which have been reported:<sup>[22]</sup>  $[Gd_4(\mu_3-OH)_2(L)_2L_1L_2(HOCH_3)_2] \cdot 11H_2O$   $\{H_2L = 2,3-bis((E)-(2-hydroxy-3-methoxy benzylidene) amino) maleonitrile, HL_1 = (2-amino-3-((E)-(2-hydroxy-3-methoxy benzylidene)amino)maleonitrile), H_3L_2 = ((1E,3Z,8Z,10E)-1,6,11-tris(2-hydroxy-3-methoxyphenyl)-2,5,7,10-tetraazaundeca-1,3,8,10-tetraene-3,4,8,9-tetracarbonitrile), -\Delta S_m = 27.2 J kg^{-1} K^{-1}$  for  $\Delta H = 7$  T at 3 K};  $[Ln_4L_4(OH)_2](OAc)_2 \cdot 4H_2O$   $\{H_2L = butanedihydrazidebridged bis(3-ethoxysalicylaldehyde) ligand, -\Delta S_m = 24.4 J kg^{-1} K^{-1}$  for  $\Delta H = 7$  T at 3 K}. For **1**, the smaller  $-\Delta S_m$  is mainly due to the relatively larger magnetic density ( $M_W/N_{Gd}$  ratio,  $M_W/N_{Gd} = 721.4$ ).

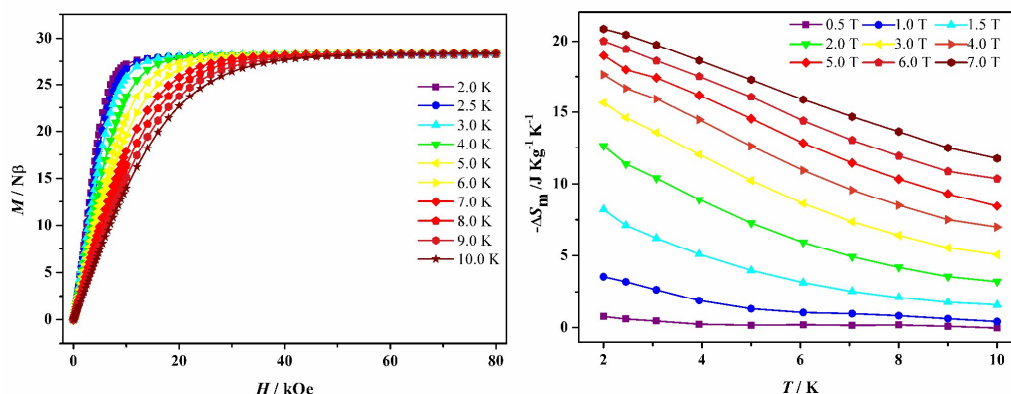


Figure 3. (Left)  $M$  versus  $H$  plots for **1** at  $T = 2.0$ – $10.0$  K and  $H = 0$ – $80$  kOe. (Right) Temperature dependence of magnetic entropy change ( $-\Delta S_m$ ) as calculated from the magnetization data of **1** at  $T = 2$ – $10.0$  K and  $0$ – $7$  T.

In order to investigate the dynamics of magnetization, the temperature dependences alternating current (AC) magnetic measurements on **3** have been performed with a 3 Oe ac magnetic field and under 0 dc field. The measurement was made in the 111–2311 Hz frequency range and at temperatures between 2 and 20 K (Figure 4), and compound **3** displays clear both in phase ( $\chi'$ ) and out-of-phase ( $\chi''$ ) ac susceptibility signals at low temperature, which is the typical of slow relaxation of the magnetization.

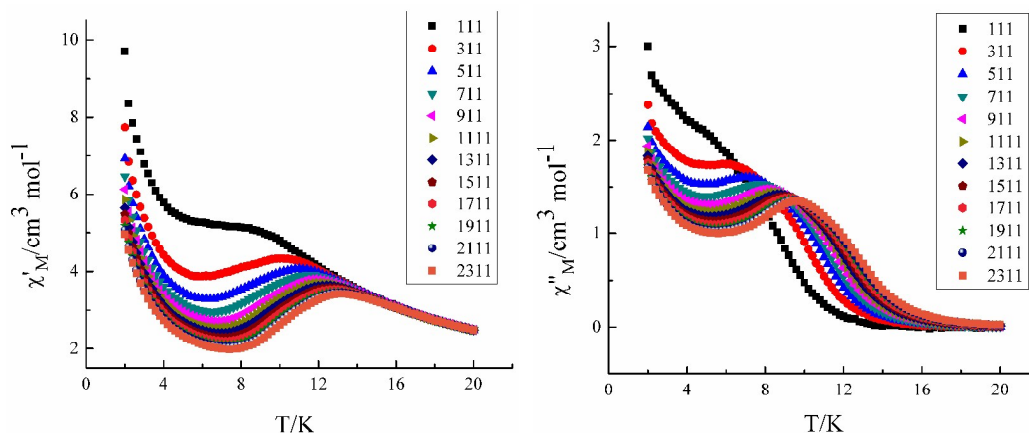


Figure 4 Temperature dependence of the in-phase ( $\chi'$ ) and out-of-phase ( $\chi''$ ) ac susceptibilities for **3** in  $H_{dc} = 0$  Oe with an oscillation of 3.0 Oe.

In addition, to further probe the dynamics of magnetization of **3**, frequency sweeping ac susceptibilities (Figure 5) were measured at 2-10 K under the zero dc fields, and the shape and frequency dependence further confirm the presence of single-molecule magnet behavior in **3**. The Cole – Cole plots of **3** are shown in Figure 7. A generalized Debye model was used in an attempt to fit the Cole-Cole diagram of **3** (Figure 6), and in the temperature range 3-10 K,  $\alpha$  parameters are in the range of 0.32–0.68. The relatively large distribution coefficients  $\alpha$  of the  $Dy_4$  complexes indicate that there is a wide distribution of relaxation time in **3**.<sup>[23]</sup> In fact, the plots at low temperature, especially at 2 K, cannot be well fitted by the generalized Debye functions. The clear distortion of the semicircle below 5 K indicates that another low temperature relaxation process might start to occur in this system below 5 K.

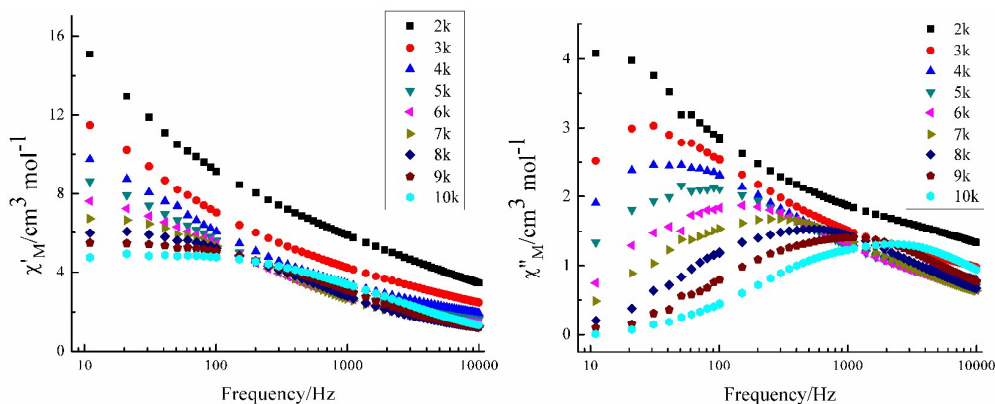


Figure 5. Frequency dependence of the in-phase ( $\chi'$ ) and out-of-phase ( $\chi''$ ) ac susceptibilities for **3**

at 2.0–10.0 K in  $H_{dc} = 0$  Oe.

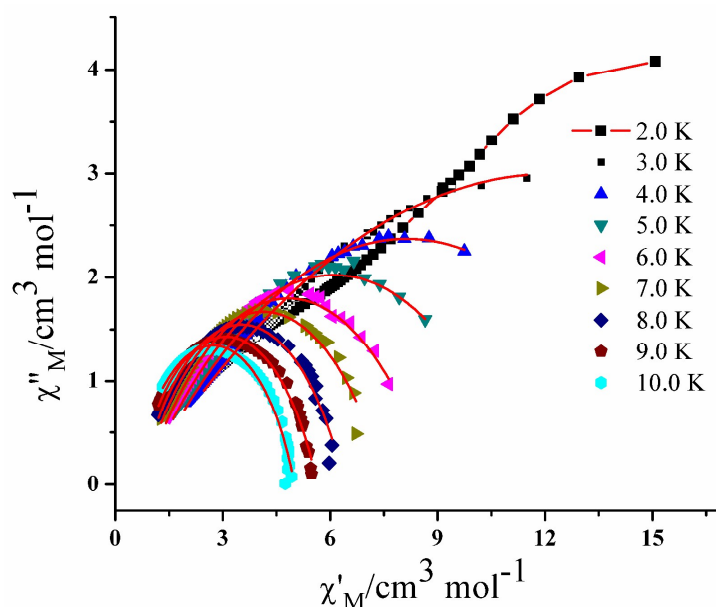
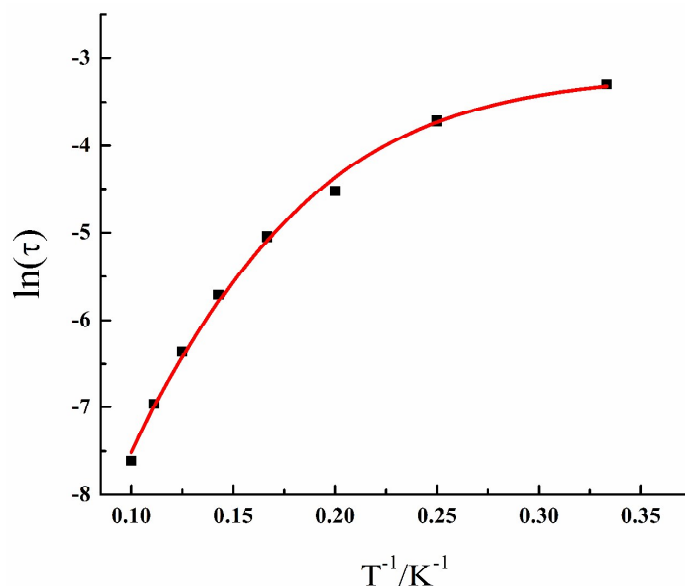


Figure 6. The cole-cole plot at different temperature in  $H_{dc} = 0$  Oe.

The Arrhenius plot exhibit an obvious curvature (Figure 7), indicating that a combination of the relaxation pathways has to be taken into account so as to understand the relaxation behavior. Data in the entire 3–10 K temperature range were analyzed by using the following equation:<sup>[24]</sup>

$$\ln \tau = -\ln[AT^m + B + CT^n + \tau_0^{-1} \exp(-U_{\text{eff}}/k_B T)]$$

where  $AT^m + B$ ,  $CT^n$ , and  $\tau_0^{-1} \exp(U_{\text{eff}}/k_B T)$  represent direct, Raman, and Orbach relaxation processes, respectively. Least-squares fitting of  $\ln \tau$  versus  $T^{-1}$  leads to  $A = 0.3759$ ,  $n = 5.02$ ,  $C = 0.0171$ ,  $U_{\text{eff}} = 45.7\text{K}$ ,  $\tau_0 = 1.23 \times 10^{-7}$  s and the agreement factor  $R$ , defined as  $R = \sum(\chi_{\text{obsd}} - \chi_{\text{calcd}})^2 / \sum(\chi_{\text{obsd}})^2$ , is  $9.39 \times 10^{-3}$ . The obtained anisotropic energy barrier ( $U_{\text{eff}}$ ) and pre-exponential factor ( $\tau_0$ ) is comparable to those previously reported for Dy-based compounds.<sup>[22,23c]</sup>



**Figure 7.**  $\ln\tau$  versus  $T^{-1}$  plots for **3**. The red solid lines represent the least-squares fits of the experimental data to the Arrhenius law.

## Conclusions

In summary, four lanthanide coordination complexes based on 8-hydroxyquinolin derivatives have been constructed and structurally characterized. Systematic magnetic studies for them have been performed, **1** exhibits cryogenic magnetic refrigeration property with  $-\Delta S_m = 20.85 \text{ J K}^{-1} \text{ kg}^{-1}$  for a field change  $\Delta H = 7 \text{ T}$  at  $2.0 \text{ K}$ . Compound **3** exhibits slow relaxation of the magnetization with  $U_{\text{eff}} = 45.7 \text{ K}$  and the preexponential factor  $\tau_0 = 1.23 \times 10^{-7} \text{ s}$ .

## Acknowledgments

We gratefully acknowledge the National Natural Science Foundation of China (21501043).

## References

- [1] (a) Y. Cui, Y. Yue, G. Qian, B. Chen, *Chem. Rev.*, 2012, **112**, 1126; (b) S. K. Sahoo, D. Sharma, R. K. Bera, G. Crisponic, J. F. Callan, *Chem. Soc. Rev.*, 2012, **41**, 7195; (c) J. Feng, H. J. Zhang, *Chem. Soc. Rev.*, 2013, **42**, 387; (d) S. Gai, C. Li, P. Yang, J. Lin, *Chem. Rev.*, 2014, **114**, 2343; (e) H. Xu, H. C. Hu, C. S. Cao, B. Zhao, *Inorg. Chem.*, 2015, **54**, 4585.

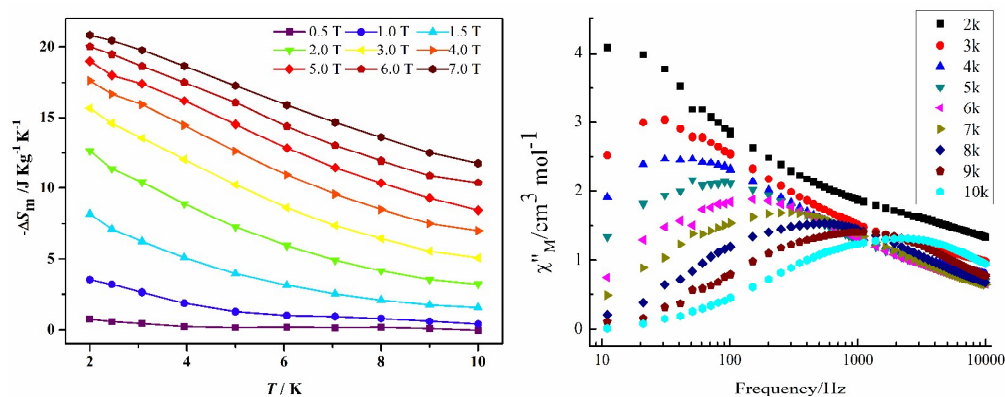
- [2] (a) D. N. Woodruff, R. E. P. Winpenny, R. A. Layfield, *Chem. Rev.*, 2013, **113**, 5110; (b) P. Zhang, Y. N. Guo, J. Tang, *Coord. Chem. Rev.*, 2013, **257**, 1728; (c) Y. Z. Zheng, Z. Zheng, X. M. Chen, *Coord. Chem. Rev.*, 2014, **258-259**, 1; (d) W. M. Wang, H. X. Zhang, S. Y. Wang, H. Y. Shen, H. L. Gao, J. Z. Cui, B. Zhao, *Inorg. Chem.*, 2015, **54**, 10610; (e) Y. X. Chang, W. M. Wang, R. X. Zhang, H. Y. Shen, X. P. Zhou, N. N. Wang, J. Z. Cui, H. L. Gao, *New J. Chem.*, 2017, **41**, 6251; (f) X. Y. Chu, H. X. Zhang, Y. X. Chang, Y. Y. Nie, J. Z. Cui, H. L. Gao, *New J. Chem.*, 2018, **42**, 5688.
- [3] (a) M. P. Suh, H. J. Park, T. K. Prasad, D.-W. Lim, *Chem. Rev.*, 2012, **112**, 782; (b) K. Sumida, D. L. Rogow, J. A. Mason, T. M. McDonald, E. D. Bloch, Z. R. Herm, T.-H. Bae, J. R. Long, *Chem. Rev.*, 2012, **112**, 724; (c) R. B. Getman, Y.-S. Bae, C. E. Wilmer, R. Q. Snurr, *Chem. Rev.*, 2012, **112**, 703; (d) J. R. Li, J. Sculley, H.-C. Zhou, *Chem. Rev.*, 2012, **112**, 869; (e) M. F. de Lange, K. J. F. M. Verouden, T. J. H. Vlucht, J. Gascon, F. Kapteijn, *Chem. Rev.*, 2015, **115**, 12205.
- [4] (a) V. S. Thoi, Y. Sun, J. R. Long, C. J. Chang, *Chem. Soc. Rev.*, 2013, **42**, 2388; (b) A. Sartorel, M. Bonchio, S. Campagna, F. Scandola, *Chem. Soc. Rev.*, 2013, **42**, 2262; (c) M. Yoon, R. Srirambalaji, K. Kim, *Chem. Rev.*, 2012, **112**, 1196.
- [5] (a) X.-Y. Wang, C. Avendaño, K. R. Dunbar, *Chem. Soc. Rev.*, 2011, **40**, 3213; (b) S. J. Liu, J. P. Zhao, W. C. Song, S. D. Han, Z. Y. Liu, X. H. Bu, *Inorg. Chem.*, 2013, **52**, 2103.
- [6] (a) Y.-Z. Zheng, G.-J. Zhou, Z. Zheng, R. E. P. Winpenny, *Chem. Soc. Rev.*, 2014, **43**, 1462; (b) S. J. Liu, C. Cao, C. C. Xie, T. F. Zheng, X. L. Tong, J. S. Liao, J. L. Chen, H. R. Wen, Z. Chang, X. H. Bu, *Dalton Trans.*, 2016, **45**, 9209; (c) S. J. Liu, C. Cao, S. L. Yao, T. F. Zheng, Z. X. Wang, C. Liu, J. S. Liao, J. L. Chen, Y. W. Li, H. R. Wen, *Dalton Trans.*, 2017, **46**, 64.
- [7] R. Sessoli, D. Gatteschi, A. Ganeschi, M. A. Novak, *Nature*, 1993, **365**, 141.
- [8] (a) D. Gatteschi, R. Sessoli and J. Villain, *Molecular Nanomagnets*, 2006; (b) L. Bogani and W. Wernsdorfer, *Nature Mater.*, 2008, **7**, 179; (c) M. Mannini, F. Pineider, P. Saintavirt, C. Danieli, E. Otero, C. Sciancalepore, A. M. Talarico, M.-A. Arrio, A. Cornia, D. Gatteschi and R. Sessoli, *Nature Mater.*, 2009, **8**, 194.
- [9] (a) M. N. Leuenberger, D. Loss, *Nature*, 2001, **410**, 789; (b) J. Lehmann, A. Gaita-Arino, E. Coronado and D. Loss *Nature Nanotech.*, 2007, **2**, 312; (c) M. Ganzhorn, S. Klyatskaya, M. Ruben, W. Wernsdorfer, *Nature. Nanotech.*, 2013, **8**, 165.
- [10] J. Liu, Y. C. Chen, J. L. Liu, V. Vieru, L. Ungur, J. H. Jia, L. F. Chibotaru, Y. Lan, W. Wernsdorfer, S. Gao, X. M. Chen, M. L. Tong, *J. Am. Chem. Soc.*, 2016, **138**, 5441.
- [11] (a) Y. S. Ding, N. F. Chilton, R. E. P. Winpenny, Y. Z. Zheng, *Angew. Chem., Int. Ed.*, 2016, **55**, 16071; (b) F.-S. Guo, B. M. Day, Y.-C. Chen, M.-L. Tong, A. Mansikkamäki, R. A. Layfield, *Angew. Chem. Int. Ed.*, 2017, **56**, 11445.
- [12] (a) S. K. Langley, B. Moubaraki, C. Tomasi, M. Evangelisti, E. K. Brechin, K. S. Murray, *Inorg. Chem.*, 2014, **53**, 13154; (b) L.-X. Chang, G. Xiong, L. Wang, P. Cheng, B. Zhao, *Chem. Commun.*, 2013, **49**, 1055; (c) X.-Y. Zheng, S.-Q. Wang, W. Tang, G.-L. Zhuang, X.-J. Kong, Y.-P. Ren, L.-S. Long, L.-S. Zheng, *Chem. Commun.*, 2015, **51**, 10687.
- [13] (a) J.-B. Peng, X.-J. Kong, Q.-C. Zhang, M. Orendáč, J. Prokleška, Y.-P. Ren, L.-S. Long, Z.-P. Zheng, L.-S. Zheng, *J. Am. Chem. Soc.*, 2014, **136**, 17938; (b) Y.-Z. Zheng, M. Evangelisti, F. Tuna, R. E. P. Winpenny, *J. Am. Chem. Soc.*, 2012, **134**, 1057.
- [14] (a) Y. C. Chen, L. Qin, Z. S. Meng, D. F. Yang, C. Wu, Z. D. Fu, Y. Z. Zheng, J. L. Liu, R.



- Tarasenko, M. Orendáč, J. Prokleška, V. Sechovský, M. L. Tong, *J. Mater. Chem. A*, 2014, **2**, 985; (b) S. Biswas, H. S. Jena, A. Adhikary, S. Konar, *Inorg. Chem.*, 2014, **53**, 3926.
- [15] (a) G. M. Sheldrick SHELXS-97, Program for the solution of crystal structure refinement. Germany: University of Göttingen, 1990; (b) G. M. Sheldrick SHELXTL-97, Program for X-ray crystal structure. Germany: University of Göttingen, 1997.
- [16] (a) S. Bala, M. S. Bishwas, B. Pramanik, S. Khanra, K. M. Fromm, P. Poddar, R. Mondal, *Inorg. Chem.*, 2015, **54**, 8197; (b) B. H. Koo, K. S. Lim, D. W. Ryu, W. R. Lee, E. K. Kohband, C. S. Hong, *Dalton Trans.*, 2013, **42**, 7204.
- [17] (a) S. W. Zhang, Y. Wang, J. W. Zhao, P. T. Ma, J. P. Wang, J. Y. Niu, *Dalton Trans.*, 2012, **41**, 3764; (b) S. W. Zhang, J. W. Zhao, P. T. Ma, H. N. Chen, J. Y. Niu, J. P. Wang, *Cryst. Growth Des.* 2012, **12**, 1263.
- [18] (a) A. Panagiotopoulos, T.F. Zafiropoulos, S.P. Perlepes, E. Bakalbassis, I. Masson-Ramade, O. Kahn, A. Terzis, C.P. Raptopoulou, *Inorg. Chem.* 34 (1995) 4918; (b) Z.H. Zhang, Y. Song, T. Okamura, Y. Hasegawa, W.Y. Sun, N. Ueyama, *Inorg. Chem.* 45 (2006) 2896.
- [19] (a) I. Nemec, M. Machata, R. Herchel, R. Bočab, Z. Trávníček, *Dalton Trans.* 2012, **41**, 14603; (b) Y. G. Huang, F. J. Jiang, D. Q. Yuan, M. Y. Wu, Q. Gao, W. Wei, M. C. Hong, *Cryst. Growth Des.*, 2008, **8**, 166.
- [20] M. Evangelisti, A. Candini, A. Ghirri, M. Affronte, E. K. Brechin, E. J. L. McInnes, *Appl. Phys. Lett.* 2005, **87**, 072504.
- [21] (a) L. X. Chang, G. Xiong, L. Wang, P. Cheng, B. Zhao, *Chem. Commun.* 2013, **49**, 1055; (b) G. Xiong, H. Xu, J. Z. Cui, Q. L. Wang, B. Zhao, *Dalton Trans.* 2014, **43**, 5639.
- [22] 21(a) J. A. Sheikh, A. Adhikary, S. Konar, *New J. Chem.* 2014, **38**, 3006; (b) A. K. Mondal, H. S. Jena, A. Malviya, S. Konar, *Inorg. Chem.* 2016, **55**, 5237.
- [23] (a) M. Guo, Y.-H. Xu, J.-F. Wu, L. Zhao, J.-K. Tang, *Dalton Trans.*, 2017, **46**, 8252; (b) P.-P. Cen, S. Zhang, X.-Y. Liu, W.-M. Song, Y.-Q. Zhang, G. Xie, S.-P. Chen, *Inorg. Chem.*, 2017, **56**, 3644; (c) L. Zhang, P. Zhang, L. Zhao, J.-F. Wu, M. Guo, J.-K. Tang, *Inorg. Chem.*, 2015, **54**, 5571.
- [24] (a) K. R. Meihaus, S. G. Minasian, W. W. Lukens, Jr., S. A. Kozimor, D. K. Shuh, T. Tylliszczak, J. R. Long, *J. Am. Chem. Soc.*, 2014, **136**, 6056; (b) J.-L. Liu, K. Yuan, J. D. Leng, L. Ungur, W. Wernsdorfer, F.-S. Guo, L. F. Chibotaru, M.-L. Tong, *Inorg. Chem.*, 2012, **51**, 8538.



## Table of contents



Four Tetra-nuclear lanthanide complexes were fabricated and structurally characterized. **1**-Gd exhibits cryogenic magnetic refrigeration property and **3**-Dy displays slow relaxation of the magnetization.